Reliability of RC shear walls with uncertainty of failure mode

Dong Xiang
PhD Student, College of Civil Engineering, Tongji University, Shanghai, China

Xiangling Gao
PhD, College of Civil Engineering, Tongji University, Shanghai, China

ABSTRACT: The propagation of damage evolution at different scales leads to the uncertainty of failure mode for shear walls, and it is difficult to determine the reliability of shear walls with shear failure accurately using the threshold value of flexural failure. In this study, the feasibility of three-parameter kinematic theory for shear-dominated reinforced concrete shear walls is validated by the shear capacity of 27 RC shear walls and the lateral load-displacement curves of 8 RC shear walls. The deterministic and stochastic parametric analysis of shear walls' nonlinear behavior are conducted, and the results indicate that multiple failure modes occur in shear walls with compressive strength of concrete 44-64MPa. Finally, the damage state is chosen as the failure threshold, and the calculation results indicate that the reliability of RC shear walls under major earthquake was improved by increasing the compressive strength of concrete.

The shear walls with stochastic dimensions and materials properties experience catastrophic dynamic effects with significant randomness in terms of time, location and amplitude during their service period (Roberts and Spanos 2003). Uncertainty in the failure mode for shear walls is caused by the propagation of damage at different scales. The threshold value of flexure failure makes it inaccurate to assess the shear wall's reliability with shear failure. Therefore, it has important theoretical significance and practical value of engineering to examine the reliability of shear walls under multiple failure using a methodology with clear physical meaning.

The unified theory of concrete structures (Hsu and Mo 2010) has made significant advancements in understanding the ultimate bearing capacity and failure modes of structural components. The shear failure is essentially a two-dimensional problem, and it has taken a long time to develop the mechanical mechanism and failure criterion of shear failure. Modified compression field theory (Vecchio and Collins 1986) and softened membrane model (Hsu and Zhu 2002) are examples of mesoscopic shear theory, while multiple vertical line element model (Vulcano *et al*. 1988) and strut-and-tie model (Zhao *et al*. 2018) are representative examples of macroscopic modes of shear walls.

The average force-deformation response has been established empirically by taking into account the effects of strain or stress at cracks and between cracks, as well as bond slip and shear slip at cracks within the framework of mesoscopic shear theory. The force transfer path is assumed for shear walls within the framework of macroscopic shear model, resulting in its mechanical mechanism to be ambiguous. Mihaylov *et al*. (2016, 2019) recently developed a kinematics-based method for studying the shear behavior of RC components, which allows for accurate simulation of the force-displacement response of RC members under disturbed stresses.

The coupling effect between nonlinearity and randomness brought attention to the necessary to incorporate reliability index into the structural analysis. Li *et al*. (2004, 2017) proposed a probability density evolution method for compound random vibration analysis of stochastic structures. The augmented state vector is introduced to construct a state equation with random initial conditions. The governing equation for the response of compound random vibrations is deduced and solved with the precise integration method and various difference schemes.

The combination explosion problem in the conventional global reliability analysis of engineering structures is dissolved by the equivalent extreme-value event (Li *et al*. 2007, Chen and Li 2007). The physically-based synthesis method integrates the physical and mechanical mechanisms, the physical failure criteria and the propagation law of randomness inherent in physical systems (Li 2018). The rationality of the aforementioned physical failure criteria depends on the establishment of an accurate physical model. At the component level, the propagation of damage evolution at different scales and the competing mechanism of several failure modes (such as flexural failure, shear failure) results in the uncertainty of failure mode.

In this paper, the bearing capacity of 27 sets of RC shear walls and the load-displacement curves of 8 sets of RC shear walls are used to verify the feasibility of the kinematics-based approach. The stochastic fluctuation of nonlinear response of RC shear walls is proved to be caused by the randomness of the axial force, structure dimensions and material properties. The coefficient of variation of ultimate bearing capacity, residual bearing capacity and their corresponding deformation are quantified. The calculation results indicate that increasing the concrete strength can improve the reliability of RC shear walls under major earthquakes.

1. SHEAR MODEL BASED ON KINEMATIC PRINCIPLE

The application of the three-parameter kinematic theory for shear-dominated RC shear walls (Mihaylov *et al*. 2016) was constrained by the assumptions regarding its displacement field and failure state: (1) the axial load ratio $N/bhf'_c < 0.2$; (2) an aspect ratio ≤ 3.0; (3) normal strength concrete, that is $f'_c \leq 60$MPa; (4) a wall-height-to-thickness ratio ≤ 25; (5) no lap-splices in the base section and no diagonal shear reinforcement. The authors' investigation (Gao *et al*. 2021) of the shear behavior of RC coupling beams indicates that the kinematic-based approach is valid even when the concrete compressive strength and aspect ratio are 80MPa and 3.5, respectively.

1.1. Calculation method of shear walls

1.1.1. Displacement fields

The displacement fields of the RC shear walls is primarily determined by the average longitudinal reinforcement strain $\varepsilon_{t,avg}$, the horizontal shear deformation Δ_c, and the vertical deformation Δ_{cx} in the shear compression zone. Thus, the displacement fields of uncracked shear walls are expressed as: $\delta_x(x, z) = f_1(\varepsilon_{t,avg}, \Delta_{cx})$, $\delta_z(x, z) = f_2(\varepsilon_{t,avg}, \Delta_{cx}, \Delta_c)$; and the displacement fields of cracked shear walls are expressed as: $\delta_x(x, z) = f_3(\varepsilon_{t,avg})$, $\delta_z(x, z) = f_4(\varepsilon_{t,avg})$. (Figure 1)

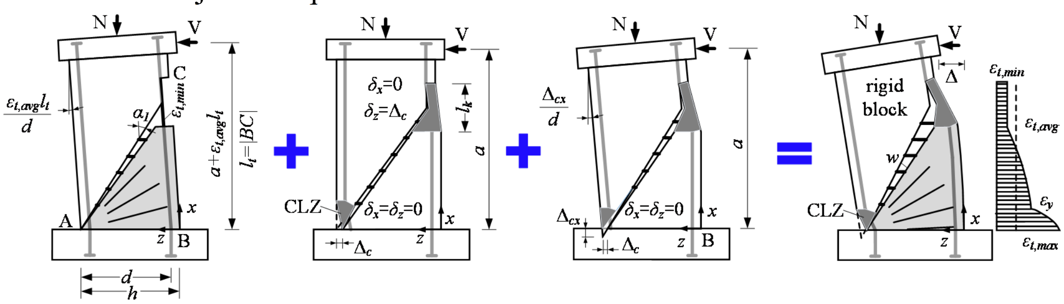

Figure 1: Deformation patterns and DOFs of RC shear wall (*Mihaylov et al. 2016*)

1.1.2. Geometrical parameters

The expression for characteristic length l_{b1e} of shear compression zone is:

$$l_{b1e} = 0.11\sqrt{a^2 + h^2} \leq 370\text{mm} \quad (1)$$

The angle of inclined crack is calculated according to simplified modified compression field theory proposed by Bentz *et al*. (2006):

$$\alpha_1 = \left(29 + 7000\varepsilon_x\right)\left(0.88 + \frac{s_{xe}}{2500}\right) \leq 75^\circ \quad (2)$$

where normal strain ε_x at the half section height and crack spacing parameters s_{xe} are calculated according to AASHTO (2007).

Length of transition zone between fan-shaped zone and rigid block is calculated as follows:

$$l_k = l_0 + \min\left[s_{cr}, d\left(\cot\alpha - \cot\alpha_1\right)\right] \quad (3)$$

Cracked length along longitudinal reinforcement is calculated as follows:

$$l_t = d\cot\alpha_1 + \left(l_k - l_0\right) \quad (4)$$

1.1.3. Shear mechanism

The shear mechanism of RC shear walls can be represented by a set of nonlinear spring, and the shear capacity provided by shear compression zone is determined as follows:

$$F_{CLZ} = \alpha l_{b1e} b f_{c,CLZ}\left(\varepsilon_{CLZ}\right) \quad (5)$$

where $f_{c,CLZ}$ is the stress-strain relationship of concrete, and Popovics' model (1970) and Mander's model (1988) are used for unconfined concrete and confined concrete, respectively.

The aggregate interlock force is calculated as follows:

$$F_{ci} = 0.18 v_{ci}\left(\Delta_{ci}, w\right) b d_1 / \sin\alpha_1 \quad (6)$$

where Li's model (1989) is adopted to calculated the aggregate interlock shear stress v_{ci}.

The force in the stirrups is calculated according to Eq. (7):

$$F_s = A_v f_v\left(\varepsilon_v\right) \quad (7)$$

Where $A_v = \rho_v b \cdot \max[d_1\cot\alpha_1 - 1.5 l_{b1e} - l_0(d/d_1), 0.5 d_1\cot\alpha_1]$.

The dowel action force is calculated as follows:

$$F_d = \frac{12 n_b E_s \pi d_b^4 \Delta d}{64 l_k^3} \leq \frac{n_b f_y d_b^3}{3 l_k}\left[1 - \left(\frac{F_{t,min}}{f_y A_s}\right)^2\right] \quad (8)$$

The lateral displacement Δ, the vertical displacement Δ_{cx}, and the rotation θ of uncracked shear wall are adopted as numerical degrees of freedom. The displacement method, where secant stiffness is employed for iteration, is used to investigate the shear behavior of the RC shear walls. The specific numerical algorithm is elaborated in reference (Mihaylov *et al*. 2016).

1.2. Model validation

1.2.1. Prediction of shear capacity

The feasibility of the shear model was validated by the shear capacities of 27 experimental RC shear walls in the literatures (Bimschas 2010, Hannewald *et al*. 2013, Maier and Thürlimann 1985, Pilakoutas and Elnashai 1995, Tran and Wallace 2012, Luna *et al*. 2013, Lefas *et al*. 1990, Oh *et al*. 2002). In the test dataset, the parameters of the RC shear walls satisfy the restriction on its applicability, where the aspect ratio ranges from 0.33- 3.00, the wall-height-to-thickness ratios are between 5.00- 21.20, and the axial force ratio ranges from 0- 0.1.

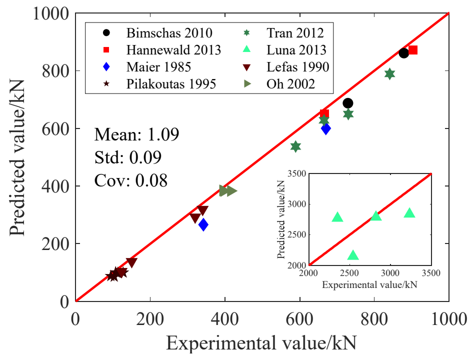

Figure 2: Experimental-to-predicted ratio of shear strength

The mean, standard deviation, and coefficient of variation of the experimental-to-predicted shear capacity ratios were found to be 1.09, 0.09 and 0.08, respectively (Figure 2). The predicted shear capacity of 23 shear walls are within the range of standard deviation, and this good agreement sufficiently demonstrates that the kinematic theory provides an accurate assessment of the shear capacity of RC shear walls.

1.2.2. Analysis of load-displacement curves

The feasibility of the shear model based on the kinematic approach to analyze the load-displacement curves is verified by eight shear walls specimens, where VK1, TW3, WR10 and WR20 are flexural failure, and VK3, VK6, VK7 and WR0 are shear failure (Figure 3). Therefore, the inherent multiple failure modes under the condition of the stochastic excitation, structure dimensions and material properties can be analyzed by the kinematic-based approach.

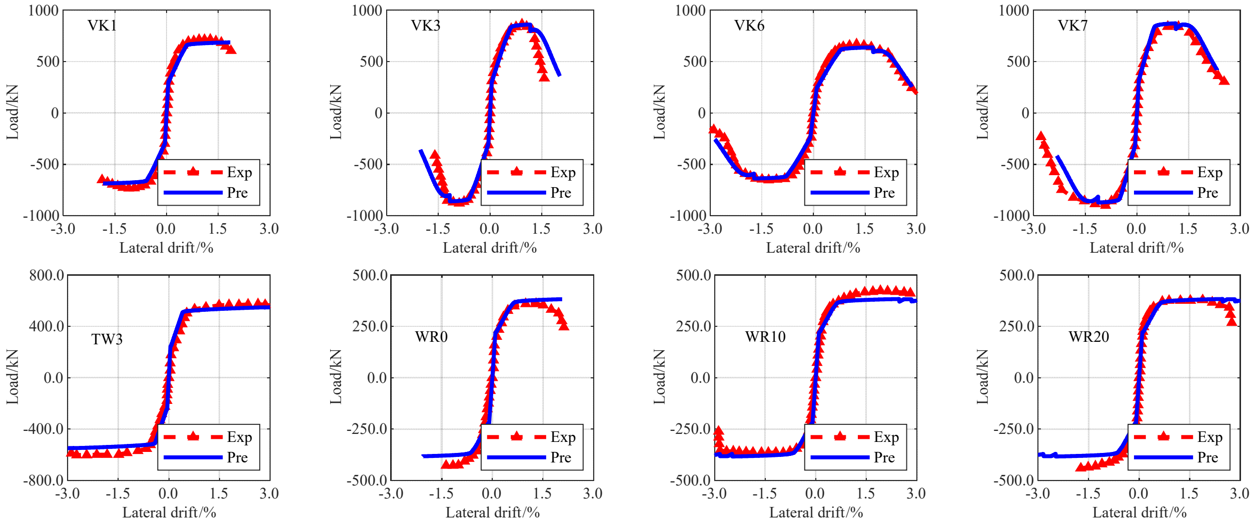

Figure 3: Experimental and predicted lateral load versus lateral drift

2. COMPOUND STOCHASTIC NONLINEAR ANALYSIS OF RC SHEAR WALLS

2.1. Deterministic parametric analysis

The compressive strength of concrete was chosen as the influencing factor to perform deterministic parametric analysis based on the seismic performance test specimen VK3 conducted by Bimschas (2010). The design concrete compressive strength is 34MPa. The load-displacement curves of test specimens with concrete compressive strength of 24MPa-74MPa are analyzed in this study. It can be concluded that the post-peak nonlinear response of the RC shear walls gradually changes from softening to ductility (Figure 4).

2.2. Stochastic parametric analysis

In this study, the axial force, structure dimensions and mechanical parameters are taken as random variables, and the experimental value is taken as the mean of each random variable while the coefficient of variation and probability distribution of random variables are determined according to JCSS (2000). In Table 1, N denotes axial force; a denotes wall height; h denotes wall width; b denotes wall thickness; d_b denotes diameter of longitudinal reinforcement; d_v denotes diameter of stirrups; E_l denotes elastic modulus of longitudinal reinforcement; f_{yl} denotes yield strength of longitudinal reinforcement; E_v denotes elastic modulus of stirrups; f_{yv} denotes yield strength of stirrups; f'_c denotes concrete compressive strength; a_g denotes diameter of aggregate.

In order to achieve good balance between accuracy and efficiency, a GF-discrepancy (Chen *et al*. 2016) for point selection is adopted and 400 samples Θ_i (i = 1, 2, ⋯, 400) are selected based on the probability distribution of random variables. After the representative points are selected, deterministic physical analysis can be carried out according to the shear model based on the kinematic approach.

The compound stochastic nonlinear analysis results of RC shear walls is presented in Figure 4. The mean and coefficient of variation of the shear capacity and corresponding displacements, as well as residual shear capacity and corresponding displacements are presented in Figure 5. When the concrete compressive strength is 44MPa, 54MPa and 64MPa, multiple failure occurs for shear walls, and the coefficient of variation of the displacement corresponding to shear capacity and the residual shear capacity reaches 0.32 and 0.29, respectively. Additionally, the designed flexural failure is changed into shear failure by introducing the randomness of excitation and material properties, and vice versa.

Table 1: Probability distribution characteristics of random sources

Random sources	Mean	Coefficient of variation	Distribution
N/kN	1300	0.1	Normal
a/mm	3300	0.001	Normal
h/mm	1500	0.001	Normal
b/mm	350	0.001	Normal
d_b/mm	14	0.001	Normal
d_v/mm	6	0.001	Normal
E_l/GPa	200	0.01	Normal
f_{yl}/MPa	515	0.01	Normal
E_v/GPa	200	0.01	Normal
f_{yv}/MPa	518	0.05	Normal
f'_c/MPa	-	0.25	Normal
a_g/mm	16	0.04	Normal

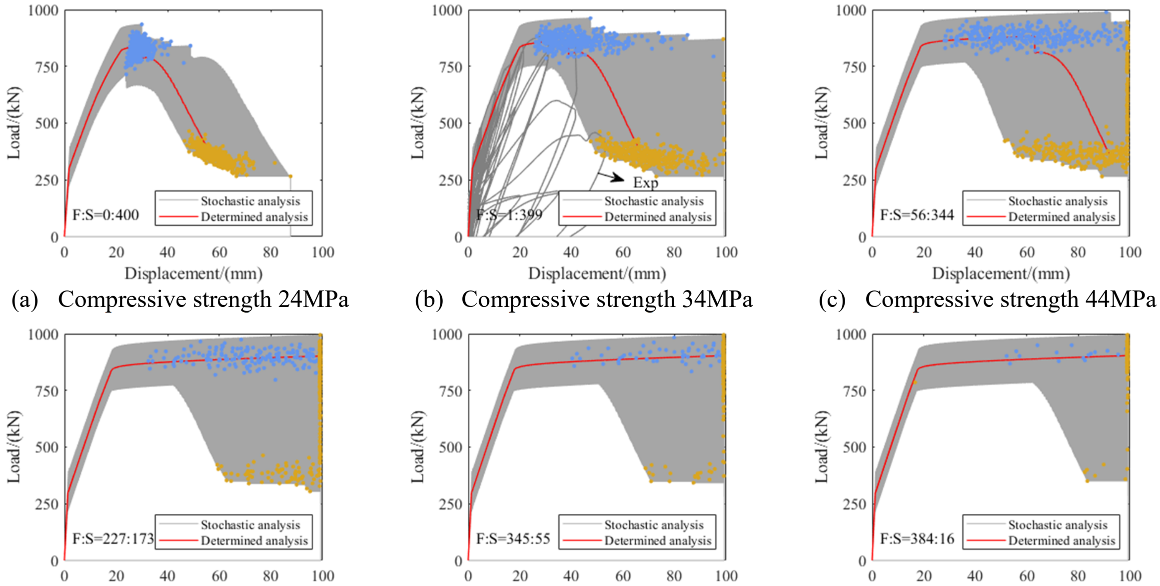

(a) Compressive strength 24MPa (b) Compressive strength 34MPa (c) Compressive strength 44MPa

(d) Compressive strength 54MPa (e) Compressive strength 64MPa (f) Compressive strength 74MPa

Figure 4: Stochastic nonlinear analysis of RC shear wall

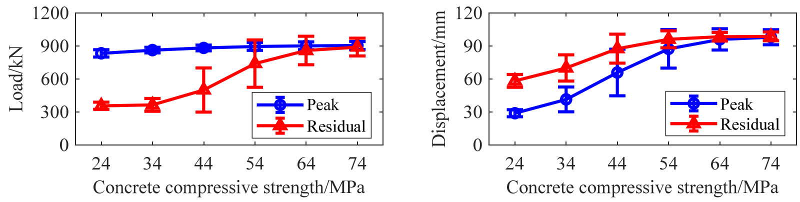

Figure 5: Statistical characteristic of key point of lateral load-displacement curves

3. PROBABILITY DENSITY EVOLUTION ANALYSIS

3.1. The generalized density evolution equation and total variation diminishing difference scheme

The principle of probability preservation occupies a fundamental role in the state evolution process of a conservative stochastic system (Li and Chen 2009). We now consider the generic stochastic dynamical system where $\boldsymbol{\Theta} = (\Theta_1, \Theta_1, \ldots, \Theta_s)$ is an s-dimensional vector characterizing the randomness and $\mathbf{Z}(t) = (Z_1(t), Z_2(t), \ldots, Z_n(t))^{\mathrm{T}}$ is an n-dimensional physical quantities associated with the system. Note that the joint PDF of system $(\mathbf{Z}, \boldsymbol{\Theta})$ is $p_{z\theta}(z, \boldsymbol{\theta}, t)$, and Eq. (9) can be derived according to random event description of the principle of preservation of probability:

$$\frac{\mathrm{D}}{\mathrm{D}t}\int_{\Omega_t\times\Omega_\Theta} p_{z\theta}\left(z,\boldsymbol{\theta},t\right)\mathrm{d}z\mathrm{d}\boldsymbol{\theta} = 0 \qquad (9)$$

After a series of mathematical operations on Eq. (9) and taking into account the arbitrariness of $\Omega_t\times\Omega_\theta$, we have:

$$\frac{\partial p_{z\theta}\left(z,\boldsymbol{\theta},t\right)}{\partial t} + \sum_{\ell=1}^{m}\dot{Z}_\ell\left(\boldsymbol{\theta},t\right)\frac{\partial p_{z\theta}\left(z,\boldsymbol{\theta},t\right)}{\partial z_\ell} = 0 \qquad (10)$$

The joint density of $\mathbf{Z}(t)$ can then be given by:

$$p_{\boldsymbol{Z}}\left(z,t\right) = \int_\Omega p_{\boldsymbol{Z\theta}}\left(z,\boldsymbol{\theta},t\right)\mathrm{d}\boldsymbol{\theta} \qquad (11)$$

The TVD difference scheme is adopted to solve the compound stochastic nonlinear analysis results of RC shear walls. Figure 6 presents the probability density evolution analysis of lateral load of RC shear walls. The probability density is relatively concentrated and the evolution trajectory is similar in the rising portion of the load-displacement curves. There is a softening trend due to the shear failure of some samples, resulting in stochastic bifurcation of the horizontal load when it exceeds the peak bearing capacity, where some probability density curves evolve in the direction of the peak bearing capacity and the other evolve in the direction of the softening of the bearing capacity.

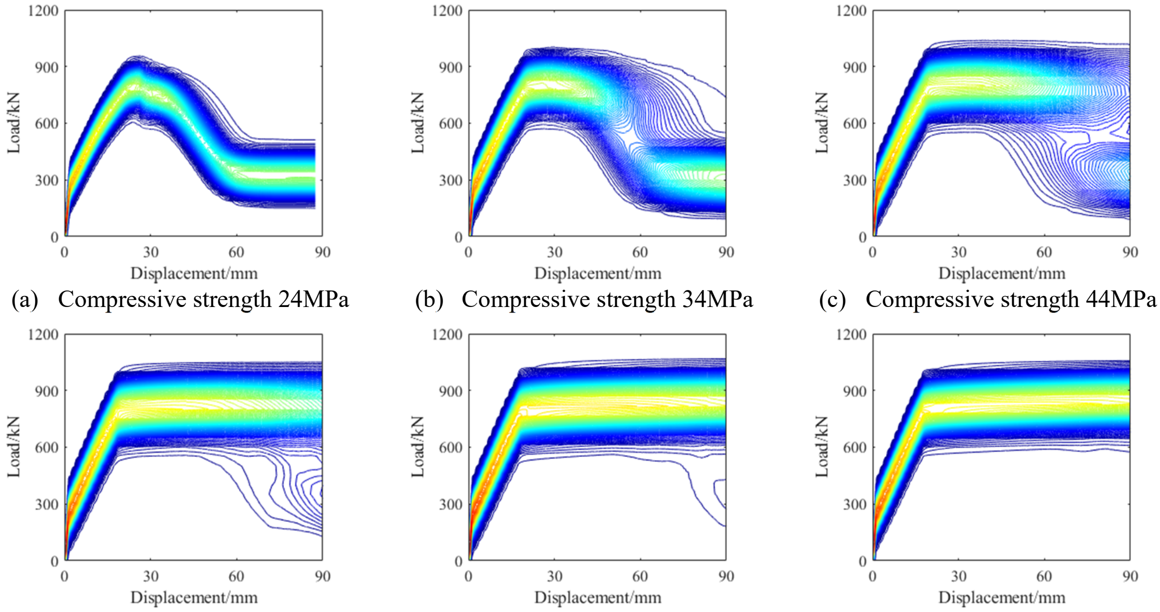

(a) Compressive strength 24MPa (b) Compressive strength 34MPa (c) Compressive strength 44MPa
(d) Compressive strength 54MPa (e) Compressive strength 64MPa (f) Compressive strength 74MPa

Figure 6: Probability density evolution analysis of lateral load of RC shear walls

When the concrete compressive strength is 24MPa, 34MPa, 64MPa and 74MPa, the probability density of lateral load is unimodal. When the concrete compressive strength is 44MPa, the design failure mode is shear failure, and the probability density branches off in the direction of the peak bearing capacity when the displacement is 45mm. The probability distribution changes from unimodal form to bimodal distribution. When the concrete compressive strength is 54MPa, the design failure mode is flexural failure, but the probability density branches off in the softening direction when the displacement is 75mm, which is detrimental to the structural safety.

3.2. Absorbing boundary condition method and reliability analysis

If a sample violates the criterion to ensure the safety of the structure, this sample will contribute to the failure probability, but not contribute to the reliability (Li and Chen 2009). Thus, equivalently, an absorbing boundary condition can be imposed on Eq. (10):

$$\breve{p}_{z\boldsymbol{\theta}}(z,\boldsymbol{\theta},t) = 0, x \in \Omega_f \tag{12}$$

Where Ω_f is the failure domain, and the remaining probability density can be calculated as follows:

$$\breve{p}_z(z,t) = \int_{\Omega_\theta} \breve{p}_{z\boldsymbol{\theta}}(z,\boldsymbol{\theta},t)\mathrm{d}\boldsymbol{\theta} \tag{13}$$

The reliability is then given by:

$$R(t) = \int_{-\infty}^{\infty} \breve{p}_z(z,t)\mathrm{d}z \tag{14}$$

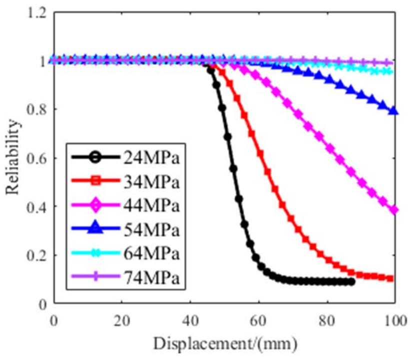

Figure 7: Reliability analysis of RC shear wall

In this study, the failure domain is defined as $\Delta > \Delta_{peak}$ and $V_{residual} < (1 - Coe) \times V_{peak}$. V_{peak} and Δ_{peak} are the peak bearing capacity and the corresponding displacement, $V_{residual}$ is the residual shear capacity and Coe is the degradation coefficient of bearing capacity. Technical specification for concrete structures of tall building (JGJ3 2010) define five component damage states, where the limit for severe damage state is the degradation of the bearing capacity by 20%. In this paper, the degradation coefficient of bearing capacity is 0.5 corresponding to the failure state. It can be concluded that increasing the concrete compressive strength can significantly increase the reliability of the shear walls under major earthquakes (Figure 7).

4. CONCLUSIONS

In this paper, the shear model of shear walls based on the kinematics principle and the probability density evolution method are used to analyze the reliability of RC shear walls with uncertainty of failure mode. The main conclusions are as follows:

1. The shear model of shear walls based on the kinematics approach has good applicability on the prediction of nonlinear behavior of shear walls.
2. The influence of randomness on the damage evolution at different scales leads to the uncertainty of failure mode for shear walls. The coefficient of variation of key point reaches about 0.3.
3. Increasing the concrete compressive strength can significantly improve the reliability of the shear walls under major earthquakes.

5. ACKNOWLEDGEMENT

This work was supported by the Tongji University (No.0200219296).

6. REFERENCES

AASHTO. (2007). *AASHTO LRFD bridge design specifications*. Washington, DC.

Bentz, E. C., Vecchio, F. J., and Collins, M. P. (2006). “Simplified modified compression field theory for calculating shear strength of reinforced concrete elements.” *ACI Materials Journal*, 103(4), 614.

Bimschas, M. (2010). “Displacement based seismic assessment of existing bridges in regions of moderate seismicity.” *ETH Zurich*.

Chen, J. B., and Li, J. (2007). “The extreme value distribution and dynamic reliability analysis of nonlinear structures with uncertain parameters.” *Structural Safety*, 29(2), 77–93.

Chen, J. B., Yang, J. Y., and Li, J. (2016). “A GF-discrepancy for point selection in stochastic seismic response analysis of structures with uncertain parameters." *Structural Safety*, 59, 20–31.

China Architecture & Building Press. (2010) *Technical specification for concrete structures of tall building: JGJ 3-2010*. Beijing. (in Chinese)

Gao, X. L., Xiang, D., Li, J., and Ren, X. D. (2021). "Decomposition of the shear capacity of steel fiber–reinforced concrete coupling beams." *Journal of Structural Engineering*, 147(11), 4021176.

Hannewald, P., Bimschas, M., and Dazio, A. (2013). "Quasi-static cyclic tests on RC bridge piers with detailing deficiencies." *ETH Zurich*.

Hsu, T. T. C., and Mo, Y. L. (2010). *Unified Theory of Concrete Structures*. John Wiley & Sons.

Hsu, T. T. C., and Zhu, R. R. H. (2002). "Softened membrane model for reinforced concrete elements in shear." *ACI Structural Journal*, 99(4), 460–469.

Lefas, I. D., Kotsovos, M. D., and Ambraseys, N. N. (1990). "Behavior of reinforced concrete structural walls: strength, deformation characteristics, and failure mechanism." *ACI Structural Journal*, 87(1), 23–31.

Li, B. (1989). "Contact density model for stress transfer across cracks in concrete." *University of Tokyo*.

Li, J. (2018). "Advances in global reliability analysis of engineering structures." *China Civil Engineering Journal*, 51(8), 1–10. (in Chinese)

Li, J., and Chen, J. B. (2004). "Probability density evolution method for dynamic response analysis of structures with uncertain parameters." *Computational Mechanics*, 34(5), 400–409.

Li, J., and Chen, J. B. (2009). *Stochastic Dynamics of Structures*. John Wiley & Sons.

Li, J., Chen, J. B., and Fan, W. L. (2007). "The equivalent extreme-value event and evaluation of the structural system reliability." *Structural safety*, 29(2), 112–131.

Luna, B., Whittaker, A., and Rivera, J. (2013). "Seismic behavior of low aspect ratio reinforced concrete shear walls." *ACI Structural Journal*, 112(5): 593-604.

Maier, J., and Thürlimann, B. (1985). "Bruchversuche an stahlbetonscheiben." *ETH Zürich*.

Mander, J. B., Priestley, M. J. N., and Park, R. (1988). "Theoretical stress-strain model for confined concrete." *Journal of Structural Engineering*, 114(8), 1804–1826.

Mihaylov, B. I. (2019). "A kinematics-based approach for the shear strength of short fibre-reinforced concrete coupling beams." *Engineering Structures*, 182, 501–509.

Mihaylov, B. I., Hannewald, P., and Beyer, K. (2016). "Three-parameter kinematic theory for shear-dominated reinforced concrete walls." *Journal of Structural Engineering*, 142(7), 4016041.

Oh, Y., Han, S. W., and Lee, L. (2002). "Effect of boundary element details on the seismic deformation capacity of structural walls." *Earthquake Engineering & Structural Dynamics*, 31(8), 1583–1602.

Pilakoutas, K., and Elnashai, A. S. (1995). "Cyclic behavior of reinforced concrete cantilever walls, Part I: Experimental results." *ACI Structural Journal*, 92(3), 271–281.

Popovics, S. (1970). "A review of stress-strain relationships for concrete." *ACI Structural Journal*, 243–248.

Probabilistic model code-Part, J. J. (2000). *3: Material properties*. Joint Committee on Structural Safety.

Roberts, J. B., and Spanos, P. D. (2003). *Random Vibration and Statistical Linearization*. Courier Corporation.

Tao, W. F., and Li, J. (2017). "An ensemble evolution numerical method for solving generalized density evolution equation." *Probabilistic Engineering Mechanics*, 48, 1–11.

Tran, T. A., and Wallace, J. W. (2012). "Experimental study of nonlinear flexural and shear deformations of reinforced concrete structural walls." *15th World Conference on Earthquake Engineering*.

Vecchio, F. J., and Collins, M. P. (1986). "The modified compression-field theory for reinforced concrete elements subjected to shear." *ACI Structural Journal*, 83(2), 219–231.

Vulcano, A., Bertero, V. V, and Colotti, V. (1988). "Analytical modeling of RC structural walls." *Proceedings of 9th World Conference on Earthquake Engineering*, 41–46.

Zhao, J., Li, K., Shen, F., Zhang, X., and Si, C. (2018). "An analytical approach to predict shear capacity of steel fiber reinforced concrete coupling beams with small span-depth ratio." *Engineering Structures*, 171, 348–361.